Talanta 122 (2014) 195–200

Contents lists available at ScienceDirect

Talanta

journal homepage: www.elsevier.com/locate/talanta

Fabrication of multiwalled carbon nanotubes–magnetite nanocomposite as an effective ultra-sensing platform for the early screening of nasopharyngeal carcinoma by luminescence immunoassay

Chia-Ching Liu [a], S. Sadhasivam [b], S. Savitha [c], Feng-Huei Lin [a,b,*]

[a] Institute of Biomedical Engineering, National Taiwan University, Taipei 100, Taiwan
[b] Institute of Biomedical Engineering and Nanomedicine, National Health Research Institutes, Miaoli 350, Taiwan
[c] Department of Biotechnology, Sree Sastha Institute of Engineering and Technology, Chennai, India

ARTICLE INFO

Article history:
Received 26 November 2013
Received in revised form
20 January 2014
Accepted 24 January 2014
Available online 31 January 2014

Keywords:
Nasopharyngeal carcinoma
Multiwalled CNTs
Fe_3O_4
Luminescent assay
Nanocomposites
Immunosensors

ABSTRACT

The hybrid nanocomposite that consists of multiwalled carbon nanotubes (MWCNTs) and magnetite (Fe_3O_4) was fabricated by chemical co-precipitation method. Briefly, CNTs were oxidized with acids to form carboxylic group and then co-precipitated with Fe_3O_4 to form CNT–Fe_3O_4 nanocomposites. The nanocomposites were characterized by SEM, HRTEM, XRD, FTIR X-ray photoelectron spectrometry (XPS) and SQUID. The XRD results indicated the high crystallinity of Fe_3O_4 nanoparticles with spinel structure and the transmission electron microscope images depicted the intercalated iron oxide magnetic particles on the surface of CNTs. The MWCNTs–Fe_3O_4 was applied as a sensing interface to perform luminescence enzyme immunoassays. Firstly, EBNA-1 antigen was immobilized onto the carboxyl group functionalized MWCNTs–Fe_3O_4, followed by binding with anti-EBNA-1 IgA antibodies. The diluted secondary antibodies (anti-human IgA-HRP) were then added to the CNTs/Fe3O4–PEG–EBNA-1–anti-EBV IgA ab complex and act as a catalyst to produce a visible light upon reaction with the substrate luminol. The formed RLU is proportional to the amount of IgA anti-EBV antiobodies on the MWCNTs. The detection limit of proposed CNTs/Fe_3O_4 based luminescence enzyme immunoassay was in the order of 0.00128 EU/mL (1:100,000 fold dilution) for the detection of anti-EBV IgA antibodies, whereas the commercial ELISA and magnetic beads' assay was accounted for up to the dilution fold of 1000 (i.e., 0.128 EU/mL). The initial findings showed that CNTs/Fe_3O_4 nanocomposites have a great potential in luminescent enzyme immunoassays and could be used as a sensing platform for the early screening of nasopharyngeal carcinoma.

1. Introduction

Carbon nanotubes (CNTs) are remarkably a new material and are defined as allotropes of carbon with a cylindrical nanostructure with diameter ~1–10 s of nm. MWCNTs are usually made from several cylindrical carbon layers with diameters in the range of 1–3 nm for the inner tubes and 2–100 nm for the outer tubes [1]. CNTs are considered as a promising nanomaterial for various biomedical applications, delivery of therapeutics [2], cancer diagnostics [3], tissue engineering, etc. The potential applications of CNTs in bio/immuno sensing are mainly due to its exceptional thermal, electrical and mechanical properties. Despite the advantages of CNTs, several limitations like toxicity and biocompatibility of CNTs still need to be evidently addressed. Non-specific binding of biomolecules on the hydrophobic nanotube surface was considered as potential disadvantage [4], however, it could be resolved by different functionalization methods. A number of different CNTs functionalization have been proposed either by covalent or non-covalent approaches. Oxidation of CNTs using strong acids is a method commonly used for generating covalent functionalization [2]. The chemical functionalization of CNTs not only offers the compatibility with the host, but also prevents agglomeration and improves the solubility in various solvents, which is an essential criterion for biosensing applications.

The carbon nanotube (CNT)/magnetic nanoparticle hybrids have gained more and more attention, due to their good stability, unique structural and excellent magnetic properties. The enormous attention behind the fabrication of Fe_3O_4 nanocomposites is mainly explained by the superparamagnetic property of iron oxides. Further, the

* Corresponding author at: Institute of Biomedical Engineering, National Taiwan University, Taipei 100, Taiwan. Tel.: +886 2 23123456x8766; fax: +886 2 23940049.
E-mail address: double@ntu.edu.tw (F.-H. Lin).

0039-9140/$ - see front matter © 2014 Elsevier B.V. All rights reserved.
http://dx.doi.org/10.1016/j.talanta.2014.01.055

superparamagnetic property of Fe_3O_4 facilitates the recovery of functionalized CNTs using an NdFeB permanent magnet. A range of CNT–magnetite inorganic hybrid materials have been developed and used for variety of applications, like, magnetic property for microscopy, in biosensors and drug delivery [5,6]. The magnetite (Fe_3O_4) nanoparticles were loaded onto the surface of CNTs by different in situ methods like chemical precipitation and solvothermal method [7,8]. The carboxylic derivative of pyrene was used as a crosslinker for the attachment of capped magnetic nanoparticles on the surface of CNT to increase the solubility of CNTs in organic solvents [9]. It was reported that hybrid materials that contain at least two nanocrystals have received considerable interest for the rapid and sensitive detection of tumor markers [10].

The concept of using nanomaterials for biosensing is, it offers great functional surface area for biomolecule loading. In addition, the unique properties of nanometerials, such as optical, electronic and mechanical, offer the fabrication of sensors with ultrasensitive detection limit. Epstein–Barr virus (EBV) infection is causatively associated with a variety of human cancers, including nasopharyngeal carcinoma (NPC) and Epstein–Barr nuclear antigen (EBNA-1), and is the only viral nuclear protein expressed in NPC able to promote oncogenesis by altering cellular properties [11]. Nasopharyngeal carcinoma (NPC) is a highly prevalent malignancy in southern China and most in Southeast Asia and North Africa [12]. Hence, it was suggested to screen anti-EBA antibody level for the early diagnosis of nasopharyngeal carcinoma. Indirect Immunofluorescence Assay (IFA) is still widely used for EBV serodiagnosis in NPC [13], but this method is time consuming and not suitable for large-scale analysis [14]. Enzyme-linked immunosorbent assay (ELISA) provides a promising alternative with potential for automation and mass screening but it lacks standardization [15]. Sensitive and simple techniques for the precise detection of clinical markers are incredibly sought in disease monitoring especially in cancers. Recently, novel immunoassay formats using carbon nanotubes based analytical techniques offering better sensitivity and practicality than other bioanalytical techniques for the ultrasensitive detection of cancer markers [16]. Fabrication of quantum dots (QD), nanocomposite and Fe_3O_4 nanoparticle combined with electrochemiluminescence (ECL) immunoassay were proposed for the ultrasensitive detection of carcinoembryonic antigen 19-9 (CA 19-9) [17]. Here, we report the synthesis of CNTs/Fe_3O_4 hybrid nanocomposites by in situ chemical co-precipitation method. The as-prepared CNT–magnetite composites were extensively characterized and applied for an effective detection of anti-EBA IgA antibodies by luminescent immunoassay. The sensitivity of CNTs/Fe_3O_4 based luminescent immunoassay was compared with the commercial ELISA and magnetic beads assay. The system capable of ultrasensitive detection of anti-EBV IgA antibodies is greatly beneficial in the primary screening of nasopharyngeal carcinoma.

2. Experimental

2.1. Materials

Multiwall carbon nanotubes (MWCNT) were purchased from Sigma Aldrich, USA, with 7–15 nm in diameter, and 0.5–200 μm in length. Ferrous chloride 4-hydrate, ferric chloride, and poly(ethylene glycol) bis(amine) (PEG) were also purchased from Sigma Aldrich, USA. Epstein–Barr nuclear antigen 1 (EBNA-1) was purchased from Development Center for Biotechnology, Taiwan. MediPro anti-EBV IgA ELISA was purchased from Formosa Biomedical Tech Corp., Taiwan. SuperSignal ELISA Pico chemiluminescent substrate was purchased from Thermo Scientific (USA). The commercial magnetic beads (Dynabeads® M-270 Carboxylic Acid) were purchased were purchased from Life Technologies (USA).

2.2. Oxidation of carbon nanotubes

400 μg of CNTs was stirred with the mixture of concentrated sulfuric acid/nitric acid (3:1) solutions and refluxed at 80 °C for 4 h to graft a carboxylic acid groups on the surface of CNTs. Followed by, the solution was diluted with 1 L of distilled water and the excessive acid was removed through a polycarbonate filter paper with 0.1 μm pore size. The prepared samples were then dried in an oven at 60 °C overnight.

2.3. Preparation of CNTs/Fe_3O_4 nanocomposites

The CNTs/Fe_3O_4 hybrid nanocomposites were prepared by in situ chemical co-precipitation of Fe^{2+} and Fe^{3+} ions (molar ratio 2:1) in alkaline solution to the MWCNTs. Briefly, the oxidized CNTs (400 μg) were first added to a 100 mL solution containing $FeCl_2 \cdot 4H_2O$ (0.10 g), $FeCl_3$ (0.16 g) and heated to 80 °C for 30 min with stirring under N_2 atmosphere. The solution was further heated at 65 °C for 30 min and the pH of the solution was adjusted to 12.0 with 2 N NaOH (3 mL) to form iron oxide precipitation. CNTs/Fe_3O_4 impurities were removed by washing several times with distilled water and the synthesized nanocomposites were collected using an NdFeB permanent magnet. The as-prepared nanocomposites were subsequently dried under vacuum and stored at room temperature. The equation of concomitant precipitation of Fe_3O_4 occurred in the above procedure was described below:

$$2Fe^{3+} + Fe^{2+} + 8NH_3\ H_2O \rightarrow Fe_3O_4 + 4H_2O + 8NH_4^+$$

2.4. Characterization

The morphologies of CNTs and CNTs/Fe_3O_4 nanocomposites were observed by scanning electron microscope (SEM, JEOL JSM-6300) at an accelerating voltage of 10 kV. Fourier transform infrared (FTIR) spectra of the samples were measured with a JASCO 4100 series spectrometer in the range of 4000–400 cm^{-1}; resolution 0.9 cm^{-1}. The X-ray diffraction patterns were collected on a Rigaku Rint-2200 diffractometer with Cu-kα ($\lambda = 1.5430$, 30 kV, 20 mA) radiation. The selected area electron diffraction (SAED) of CNT/Fe_3O_4 was performed by transmission electron microscopy (TEM) (Philips TECNA1 F20 at 220 kV). The qualitative analysis of surface elements was performed by X-ray photoelectron spectroscopy (XPS) equipped with PHI5000 Versa Probe (ULVAC-PHI, Chigasaki, Japan). A magnetic characterization was performed using an MPMS-7 magnetometer system (Quantum Design Company, San Diego, CA, USA).

2.5. Functionalization of CNTs/Fe_3O_4 nanocomposites

The as-prepared CNTs/Fe_3O_4 nanocomposites (100 μg) were conjugated with poly(ethylene glycol) bis(amine) (PEG) through EDC coupling. Briefly, CNTs/Fe_3O_4 was immersed in MES buffer with EDC (1%) for 30 min at 4 °C and the unreacted or the residual EDC in CNTs/Fe_3O_4 solution was removed by washing with distilled water. The activated CNTs/Fe_3O_4 was treated with PEG bis-amine (2%) for 1 h at room temperature. The activated carboxyl groups of CNTs/Fe_3O_4 will effectively bind to the amine groups of PEG through the formation of amide bond.

2.6. Immobilization of EBNA-1 onto CNTs/Fe_3O_4–PEG nanocomposites

The CNTs/Fe_3O_4–PEG nanocomposites were conjugated with EBNA-1 antigen via EDC coupling. In order to activate the carboxylic acid group, 20 μg of CNTs/Fe_3O_4–PEG was mixed with MES buffer containing 1% EDC. The solutions were transferred to a 96-wells

ELISA plate and incubated at 4 °C for 30 min. The unreacted EDC was removed by washing with MES buffer. Followed by, 2 μg/mL of EBNA-1 dissolved in PBS was added into each well (final concentration of EBNA-1 to CNTs/Fe_3O_4–PEG was 50 μg:1 mg, respectively) and incubated overnight at 4 °C. Then, CNTs/Fe_3O_4–PEG–EBNA-1 conjugate was collected by NdFeB permanent magnet and the supernatant was discarded. 200 μL of blocking buffer (SuperBlock, Pierce Biotechnology, USA) was then added to each well and incubated for 1 h at room temperature. After blocking, each well was washed five times with 200 μL of washing buffer (1 × TBS, 0.1 mM EDTA, 0.1% Tween 20). The EBNA-1 immobilization onto CNTs/Fe_3O_4–PEG nanocomposites was determined by BCA assay using UV–Vis spectrophotometry at OD 562 nm.

2.7. Commercial magnetic beads assay

The commercial magnetic beads, Dynabeads® M-270 carboxylic acid, were subjected to the similar modification process engaged for CNT/Fe_3O_4. In brief, 20 μg of Dynabeads was mixed with MES buffer containing 1% EDC and incubated at 4 °C for 30 min. Followed by, 2 μg/mL of EBNA-1 dissolved in PBS was added into each well (EBNA-1–Dynabeads ratio 50 μg:1 mg) and incubated overnight at 4 °C. The Dynabeads–PEG–EBNA-1 conjugate was collected by NdFeB permanent magnet and the remaining steps viz., separation and blocking were carried out as mentioned in Section 2.6. Finally, the detection of anti-EBV IgA antibodies was done according to Section 2.8.

2.8. Detection of anti-EBV IgA antibodies

After EBV-1 antigen immobilization, anti-EBV IgA antibody stock solution (128 EU/mL) was diluted to different concentrations, up to 10^6-fold (1:10, 1:100, 1:1000, 1:10,000, 1:100,000 and 1:1,000,000) with SuperBlock blocking solution and added into each well. The samples were incubated for 1 h at room temperature and washed five times with wash buffer. The diluted anti-human IgA-HRP (100 μg) was then added into each well containing CNTs/Fe_3O_4–PEG–EBNA-1–anti-EBV IgA ab and incubated for 30 min at room temperature. After incubation, the wells were washed with wash buffer (200 μL/well) for five times. Finally, 100 μL of Femto Lumino maximum sensitivity substrate solution (Thermo, USA) was added into each well and incubated for 2 min at room temperature in the dark. The signals generated from the reaction were measured at a wavelength of 425 nm by a luminometer reader (FlexStation 3, Molecular Devices). Anti-EBV IgA ELISA assay (MediPro, Formosa Medical Technology Corp., Taiwan) was employed as the positive control. The dilution buffer without anti-EBV IgA antibodies was served as the negative control.

2.9. Statistical analysis

The data was obtained from six independent experiments and each experiment was carried out thrice. A statistical analysis was performed using Student's *t* test. A *p* value of < 0.05 was considered as significant (*).

3. Results and discussion

3.1. CNTs/Fe_3O_4 characterization

3.1.1. SEM analysis

The size and morphology of CNTs and CNTs/Fe_3O_4 nanocomposites was examined by scanning electron microscopy (SEM). The SEM images revealed that the length of CNTs was 0.5–2.0 μm and the diameter was 5–10 nm (Fig. S1a). It can be seen that a significant amount of magnetite particles were layered on the surface of MWCNTs (Fig. S1b) compared to unmodified CNTs (Fig. S1a). It was further observed that the coverage of magnetite nanoparticles was dense and uniformly distributed without any clusters.

3.1.2. FTIR analysis

Fourier transform-infrared absorption spectra (FTIR) of the MWCNTs and oxidized MWCNTs are shown in Fig. 1. Compared with MWCNTs, several significant changes in the peak intensity of the oxidized MWCNTs spectrum were observed. The FTIR spectra of oxidized CNTs showed a peak intensity at 1720 cm^{-1} (C═O stretching), 1310 cm^{-1} (O–H stretching), 1056 cm^{-1} (C–O stretching) and 3400 cm^{-1} (increase in O–H stretching). The changes were possibly due to the introduction of carboxylic group by the oxidation of the CNTs. The FTIR spectra of CNTs allied with Fe_3O_4 showed the reduction in C═O stretching of CNTs/Fe_3O_4 spectrum at 1720 cm^{-1}, that designates the utilization of COOH of MWCNT by co-precipitation with Fe_3O_4 particles. This confirms the attachment of Fe_3O_4 on the surface of MWCNTs. Several studies reported that the oxidation of CNTs with acid results in significant changes of the spectrum that includes C═O stretching at 1720 cm^{-1}, O–H bending band at 1310 cm^{-1}, and the increase of O–H stretching band at 3440 cm^{-1} [18,19].

3.1.3. XRD analysis

The typical XRD pattern of unmodified CNT and CNT–Fe_3O_4 composite is shown in Fig. 2. The diffraction peak at $2\theta = 26.5°$ is recorded for unmodified CNT (002) in Fig. 2a that specifies the plane of layered and hexagonal structure of carbon nanotubes. The diffraction peaks recorded for CNT/Fe_3O_4 are $2\theta = 30.2$ (220), 35.6 (311), 43.3 (400), 57.3 (422) and 62.8 (511) displayed in Fig. 2b. The afore-stated diffraction peaks were consistent with the reflections of standard Fe_3O_4 (JCPDS no. 65-3107) and confirmed that the Fe_3O_4 was hooked onto the CNT surface. The sharp and well-resolved peaks recorded for CNT/Fe_3O_4 suggest the well crystalline nature of the as-prepared composites. The absence of any uncharacteristic peaks further suggests that the composites are free of impurities. The broad peak located at $2\theta = 26.2°$ is a characteristic of pure/unmodified CNTs (JCPDS card no. 75-1621) [20,21]. The absence of any extra uncharacteristic peak in the XRD pattern of the CNTs/Fe_3O_4 inorganic hybrid material concludes the formation of magnetite–CNT heterostructure via reduction reactions [22].

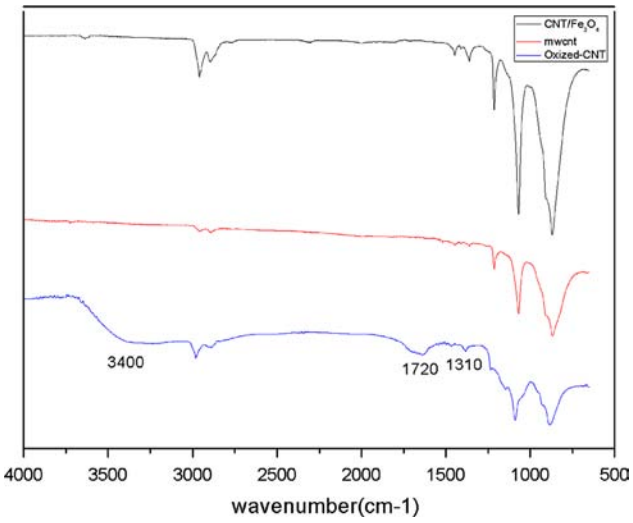

Fig. 1. FTIR spectra of MWCNT, oxidized-CNT and CNT functionalized with Fe_3O_4.

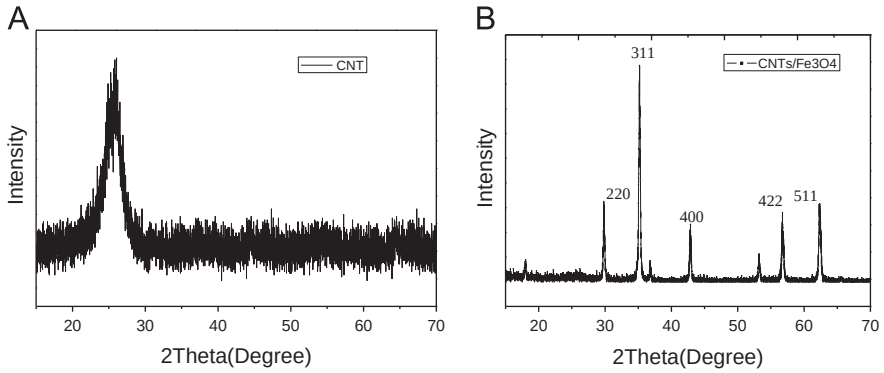

Fig. 2. XRD patterns of the (A) CNTs and (B) CNTs/Fe_3O_4 composites.

3.1.4. High-resolution transmission electron microscopy (HRTEM) analysis

The microstructure of the CNTs and CNTs/Fe_3O_4 composite was observed by high-resolution transmission electron microscopy. The HRTEM images of CNTs and CNTs/Fe_3O_4 nanocomposites are shown in Fig. S2. From Fig. S2a, it was found that the diameter of the CNT was approximately 20 nm with a clear multiwalled structure. The distribution of Fe_3O_4 nanoparticles on the MWCNTs surface accounted for narrow size distribution, uniform and dense coverage without aggregation (Fig. S2b). The average diameter of Fe_3O_4 nanoparticles was about 5 nm (Fig. S2c). The selected area electron diffraction (SAED) pattern of Fe_3O_4 nanoparticles is presented in Fig. S2d. The SAED pattern revealed a four ring pattern at (311), (422), (440), and (511) that corresponds to the planes of Fe_3O_4 as illustrated in the XRD pattern of CNTs/Fe_3O_4 composites (Fig. S2b) and concludes that the SAED pattern of CNTs/Fe_3O_4 was consistent with the XRD results. A significant amount of Fe_3O_4 nanoparticles were found on the copper grid even after washing and sonication with ethanol before TEM measurements indicate a strong affinity between pretreated MWCNTs and Fe_3O_4.

3.1.5. SQUID analysis

The magnetic hysteresis curves of CNTs, Fe_3O_4 and the CNTs/Fe_3O_4 composites are shown in Fig. 3. The CNTs without Fe_3O_4 did not show any magnetization. However, the CNTs/Fe_3O_4 composites exhibit the typical superparamagnetic properties as like Fe_3O_4. From the hysteresis curve, saturation magnetization (M_s) for CNTs/Fe_3O_4 was found to be 30 emu g^{-1}. The M_s for Fe_3O_4 was recorded as 55 emu g^{-1}. The lower saturation magnetization of CNTs/Fe_3O_4, compared to Fe_3O_4 particles might be explained by the difference in crystalline nature of CNTs/Fe_3O_4. The magnetic property of CNTs/Fe_3O_4 was significantly higher than the AuFe nanoparticles, which were reported as 13.0 emu g^{-1} and 2.5 emu g^{-1} [23,24]. The superparamagnetic nanohybrids are practical and superior to use since they do not show any spontaneous magnetic moments and do not agglomerate due to magnetic dipole–dipole interactions [25]. Furthermore, the clusters of superparamagnetic nanoparticles are effectively detached using magnetic separation [26]. The superparamagnetic property of nanocomposites is desirable for biomedical applications since it aids to prevent the aggregation of magnetic particles and enables to redisperse rapidly once the magnetic field is removed [27].

3.1.6. X-ray photoelectron spectrometry (XPS) analysis

The results of elemental composition of CNTs/Fe_3O_4 composites by XPS analysis are shown in Fig. S3. The XPS spectrum designates the characteristic peaks for carbon (C_{1s}), iron (Fe_{2p3}) and oxygen

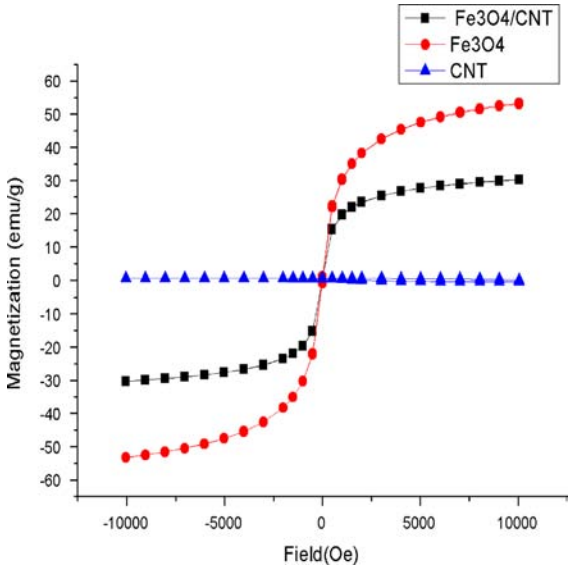

Fig. 3. Magnetization hysteresis curve of CNTs, Fe_3O_4 and CNTs/Fe_3O_4 composites.

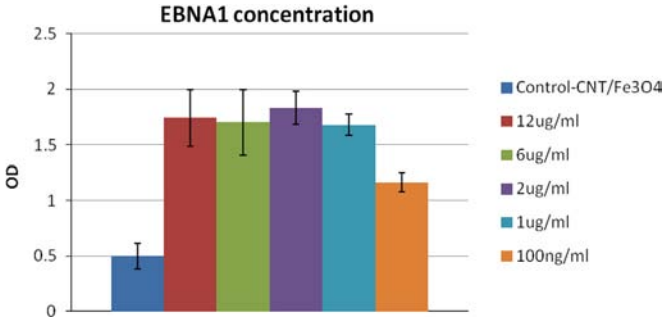

Fig. 4. Effect of different concentration of EBNA-1 antigen binding onto CNTs/Fe_3O_4 composites.

(O_{KLL}, O_{1s}), which confirms the existence of Fe_3O_4 in COOH functionalized CNT nanocomposites.

3.2. EBNA-1 immobilization onto CNTs/Fe_3O_4–PEG nanocomposites

Various concentrations of EBNA-1 antigen ranging from 100 ng/mL to 12 μg/mL (100 ng, 1, 2, 6 and 12 μg/mL) were tested to generate highly antigen functionalized surface for the sensitive detection of anti-EBA IgA antibodies in NPC positive serum. The immobilization efficiency of EBNA-1 antigen is presented in Fig. 4. This finding demonstrates 2 μg/mL of antigen can effectively bind

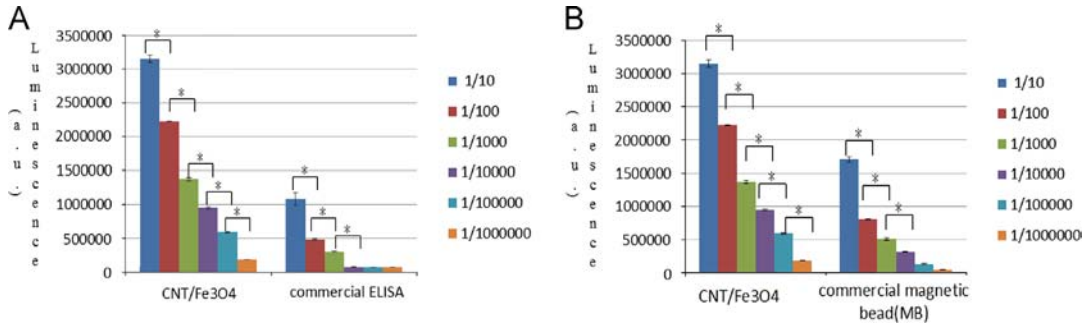

Fig. 5. Detection of different dilutions of anti-EBV IgA antibodies by CNTs/Fe_3O_4 based luminescence assay and comparison with the commercial ELISA, MediPro (A) and magnetic beads (B). (The 1/10, 1/100, 1/1000, 1/10,000, 1/100,000 and 1/1,000,000 dilutions, respectively, contain 12.8, 1.28, 0.128, 0.0128, 0.00128 and 0.000128 EU/mL of anti-EBV IgA antibodies; $^{*}p < 0.05$.)

to the CNTs/Fe_3O_4–PEG nanocomposites. Though the hydrophilicity of CNTs was considerably enhanced by the oxidation, still they tend to aggregate in most of the biological solutions due to the higher salt content [28]. It was reported that attaching hydrophilic polymers such as poly(ethylene glycol) (PEG) to oxidized CNTs will be stable in biological environments and extend the feasibility of CNTs in many in vitro and in vivo applications [29].

3.3. *Detection of anti-EBV IgA antibodies using CNTs/Fe_3O_4 based luminescence assay and comparison with commercial ELISA and magnetic beads assay*

The experiment was intended for the detection of least possible amount of anti-EBV IgA antibodies in NPC positive serum and compares the sensitivity of the CNTs/Fe_3O_4 based luminescence assay with the commercial ELISA and magnetic beads. The detection limitation and the said analytical methods were evaluated by different dilutions of anti-EBV IgA antibodies started from 1/10, 1/100, 1/1000, 1/10,000, 1/100,000 and 1/1,000,000 (12.8, 1.28, 0.128, 0.0128, 0.00128 and 0.000128 EU/mL, respectively) and the results are illustrated in Fig. 5. The CNTs/Fe_3O_4 luminescence assay had effectively detected all the concentrations of anti-EBV IgA antibodies (even up to 100,000 dilution), whereas the commercial ELISA has resulted in the possible anti-EBV IgA detection of 0.128 EU/mL (up to the dilution fold of 1000) and failed to significantly detect 0.0128 and 0.00128 EU/mL of anti-EBV IgA compared to the CNTs/Fe_3O_4 based luminescence assay (Fig. 5a). The sensitivity of commercial magnetic beads was also similar to commercial ELISA (i.e., 0.128 EU/mL) which was significantly lower than the proposed assay's lower limit of detection (LOD) of 0.00128 EU/mL (Fig. 5b). However, the magnetic beads covered by polymers are linked via a delicate physical linkage that cannot abide harsh reaction conditions like CNT–Fe_3O_4.

A general population study reported from Taiwan illustrated the screening of high titer of anti-EBV antibodies has been closely associated with the elevated risk of NPC prevalence [30] and urges the measurement of anti-EBA IgA antibodies may be useful for the early detection of nasopharyngeal carcinoma in high-risk populations. It was reported that currently there are no accepted screening tools for guiding the clinical management of individuals at high-risk for nasopharyngeal carcinomas, mostly unaffected relatives from nasopharyngeal carcinoma multiplex families [31]. We have previously reported the application of immune-PCR (iPCR) as a sensitive tool for the early screening of NPC and the sensitivity of iPCR for the detection of EBNA-1 antigen was twofold higher than the commercial ELISA kit [32]. Similarly, an ultrasensitive electrochemiluminescence immunoassay was proposed for the detection of carbohydrate antigen 19-9 (CA 19-9) using CA 19-9 Ab1/Fe_3O_4 as a capture probe and CA 19-9 Ab2/CdTe-G as a signal probe that result in the limit of detection as 0.002 pg/mL, 10^6-fold enhancement of CA 19-9 detection over the ELISA [17]. It is clear that the sensitivity of ELISA is recently outperformed by the use of CNTs in various immunoassays for the prognostic and diagnostics of various cancers and it could be possibly explained by high surface area of CNTs which in turn offers highly dense coverage of antigen or antibodies on their surface with relatively a minimum amount.

4. Conclusion

The luminescence based detection of anti-EBV IgA antibodies in NPC positive serum was effectively accomplished using CNTs/Fe_3O_4 nanocomposites. Fabrication and exploitation of new immunoassays with the sensitive quantification of anti-EBV IgA antibodies is highly claimed for the early screening of nasopharyngeal carcinoma. The fabrication of CNTs with Fe_3O_4 results in simple functionalization with PEG and EBV and easy separation via magnetic field makes the immunoassay a very effective and rapid. The detection sensitivity of CNTs/Fe_3O_4 was noted as 0.000128 EU/mL, compared to the lower detection limit of 0.0128 EU/mL by commercial ELISA and magnetic beads immunoassay formats. It was concluded that CNTs/Fe_3O_4 based chemiluminescence assay was undeniably exceptional in the quantification of anti-EBV IgA antibodies and could be applied for the primary screening of nasopharyngeal carcinoma owing to its extremely lower detection limit than the other existing immunoassays. The clinical utility of the proposed assay will be further improved by evaluating the specificity, robustness and reproducibility of the assay.

Appendix A. Supporting information

Supplementary data associated with this article can be found in the online version at http://dx.doi.org/10.1016/j.talanta.2014.01.055.

References

[1] E. Bekyarova, Y. Ni, E.B. Malarkey, J. Biomed. Nanotechnol. 1 (2005) 3–17.
[2] C. Klumpp, K. Kostarelos, M. Prato, A. Bianco, Biochim. Biophys. Acta Biomembr. 1758 (2006) 404–412.
[3] K. Teker, R. Sirdeshmukh, K. Sivakumar, S. Lu, E. Wickstrom, H.N. Wang, Nanobiotechnology 1 (2005) 171–182.
[4] Z. Liu, S. Tabakman, K. Welsher, H. Dai, Nano Res. 2 (2009) 85–120.
[5] Z. Deng, E. Yenilmez, J. Leu, J.E. Hoffman, E.W. Straver, H. Dai, K.A. Moler, Appl. Phys. Lett. 85 (2004) 6263–6265.
[6] P. Xu, D.X. Cui, B.F. Pan, F. Gao, R. He, Q. Li, T. Huang, C.C. Bao, H. Yang, Appl. Surf. Sci. 254 (2008) 5236–5240.
[7] H.Q. Cao, M.F. Zhu, Y.G. Li, J. Solid State Chem. 179 (2006) 1208–1213.
[8] H.P. Cong, J.J. He, Y. Lu, S.H. Yu, Small 6 (2010) 169–173.
[9] V. Georgakilas, V. Tzitzios, D. Gournis, D. Petridis, Chem. Mater. 17 (2005) 1613–1617.
[10] G.K. Parshetti, F.H. Lin, R.A. Doong, Sens. Actuators B: Chem. 186 (2013) 34–43.
[11] J.Y. Cao, S. Mansouri, L. Frappier, J. Virol. 86 (2012) 382–394.

[12] T. Raab, Humana Press, N.J. Totowa, J. A. Goedert (2000) 93–111.
[13] S.F. Leung, J.S. Tam, A.T. Chan, B. Zee, L.Y. Chan, D.P. Huang, A. Van Hasselt, P. J. Johnson, Y.M. Lo, Clin. Chem. 50 (2004) 339–345.
[14] D.K. Paramita, J. Fachiroh, S.M. Haryana, J.M. Middeldorp, Clin. Vaccine Immunol. 16 (2009) 706–711.
[15] B.C. Gärtner, J.M. Fischinger, K. Roemer, M. Mak, B. Fleurent, N. Mueller Lantzsch, J. Virol. Methods 93 (2001) 89–96.
[16] S. Sadhasivam, J.C. Chen, S. Savitha, C.W. Chang, F.H. Lin, J. Mater. Sci. Mater. Med. 25 (2014) 101–111.
[17] N. Gan, J. Zhou, P. Xiong, T. Li, S. Jiang, Y. Cao, Q. Jiang, Int. J. Mol. Sci. 14 (2013) 10397–10411.
[18] Y.P. Sun, W.J. Huang, Y. Lin, K.F. Fu, A. Kitaygorodskiy, L.A. Riddle, Y.J. Yu, D.L. Carroll, Chem. Mater. 13 (2001) 2864–2869.
[19] Z. Huang, J. Li, Q.W. Chen, H. Wang, Mater. Chem. Phys. 114 (2009) 33–36.
[20] L. Kong, X. Lub, W. Zhang, J. Solid State Chem. 181 (2008) 628–636.
[21] J. Safari, Z. Zarnegar, J. Ind. Eng. Chem., http://dx.doi.org/10.1016/j.jiec.2013.10.004, in press.
[22] Y. Zhan, R. Zhao, Y. Lei, F. Meng, J. Zhong, X. Liu, Appl. Surf. Sci. 257 (2011) 4524–4528.
[23] I.C. Chiang, D.H. Chen, Adv. Funct. Mater. 17 (2007) 1311–1316.
[24] H.L. Liu, J.H. Wu, J.H. Min, Y.K. Kim, J. Appl. Phys. 103 (2008) 529–531.
[25] J. Sui, J. Li, Z. Li, W. Cai, Mater. Chem. Phys. 134 (2012) 229–234.
[26] A. Ditsch, P.E. Laibinis, D.I.C. Wang, Langmuir 21 (2005) 6006.
[27] S. Wang, H. Bao, P. Yang, G. Chen, Anal. Chim. Acta 612 (2008) 182–189.
[28] Z. Liu, S. Tabakman, K. Welsher, H. Dai, Nano Res. 2 (2009) 85–120.
[29] Z. Liu, X. Sun, N. Nakayama, H. Dai, ACS Nano 1 (2007) 50–56.
[30] Y.C. Chien, J.Y. Chen, M.Y. Liu, H.I. Yang, M.M. Hsu, C.J. Chen, C.S. Yang, N. Engl. J. Med. 345 (2001) 1877–1882.
[31] C. Chang, J. Middeldorp, K.J. Yu, H. Juwana, W.L. Hsu, P.J. Lou, C.P. Wang, J.Y. Chen, M.Y. Liu, R.M. Pfeiffer, C.J. Chen, A. Hildesheim, J. Med. Virol. 85 (2013) 524–529.
[32] T.W. Wang, H.Y. Lu, P.J. Lou, F.H. Lin, Biomaterials 29 (2008) 4447–4454.